Intermetallics 66 (2015) 77–81

Contents lists available at ScienceDirect

Intermetallics

journal homepage: www.elsevier.com/locate/intermet

Evolution of the amorphous structure in melt-spun $Ti_{50}Ni_{25}Cu_{25}$ alloy subjected to high pressure torsion deformation

D.V. Gunderov [a, d, *], V.Yu. Slesarenko [b], A.A. Churakova [a, d], A.V. Lukyanov [a], E.P. Soshnikova [a], V.G. Pushin [c], R.Z. Valiev [a, b]

[a] Ufa State Aviation Technical University, 12 K. Marx str., Ufa 450000 Russia
[b] Saint Petersburg State University, 28 Universitetskiy pr., Saint Petersburg 198504 Russia
[c] Ural Division of Russian Academy of Sciences, Institute of Metal Physics, 18 S. Kovalevskaya St., Ekaterinburg 620041, Russia
[d] Institute of Molecule and Crystal Physics RAS, 151 Prospekt Oktyabrya, Ufa, Russia

ARTICLE INFO

Article history:
Received 26 December 2014
Received in revised form
12 March 2015
Accepted 13 June 2015
Available online 6 July 2015

Keywords:
Metallic glasses (or amorphous metals)
Severe plastic deformation
Rapid solidification
Glass transition and crystallization

ABSTRACT

Peculiarities of structure and mechanical behaviour of amorphous $Ti_{50}Ni_{25}Cu_{25}$ alloy were the focus of this research. The melt-spun ribbons of amorphous $Ti_{50}Ni_{25}Cu_{25}$ were subjected to high pressure torsion (HPT) at temperatures of 20–150 °C in order to modify their structure and mechanical behaviour. Some features of obtained HPT-processed samples were compared with initial state with the help of x-ray diffraction (XRD), transmission electron microscopy (TEM) and nanohardness testing. Analysis of structural data and mechanical behaviour allowed us to assume that severe plastic deformation (SPD) processing of melt-spun $Ti_{50}Ni_{25}Cu_{25}$ alloy might lead to the formation of the structure similar to the new kind of noncrystalline state – "nanoglass" state.

© 2015 Elsevier Ltd. All rights reserved.

1. Introduction

Nanostructuring is the new and promising method of enhancing the properties of metals and alloys for advanced structural and functional applications [1]. To date, it is well established that bulk nanostructured materials (BNMs) can be produced successfully via microstructural refinement using severe plastic deformation (SPD), which is heavy straining under high imposed pressure [2–4]. SPD processing is an attractive procedure for many advanced applications as it significantly modifies microstructure and can enhance the properties of a wide range of metals and alloys [4]. It was already shown [5–11] that SPD techniques, for instance high pressure torsion (HPT) may be used to produce amorphous or amorphous-crystalline alloys. At the same time, amorphous state, produced by SPD, has some features in comparison with amorphous state, obtained by melt spinning technique [10,11]. Melt spinning is the best known method for obtaining amorphous alloys, and it allows producing amorphous alloys in the form of thin ribbons (thickness of about 50 μm) by cooling the melt jet on the surface of a rapidly rotating copper wheel. It provides the melt cooling at the rate of 10^6 K/s, whereby the crystallization processes do not have time to occur. In recent years, the method for producing amorphous "bulk metallic glasses (BMG)" based on the rapid melt cooling [12], also gained widespread.

Furthermore, just several years ago the new kind of materials, called "nanoglasses", was introduced in scientific literature [14–16]. Structural state of nanoglasses may be characterized as amorphous, but they have some features in their atomic structure, that leads to the significant difference of the physical properties and mechanical behavior in comparison with amorphous state. Nanoglasses consist of amorphous nanoclusters (size about 5 nm), separated by amorphous interfaces [13]. First nanoglasses were produced mainly by inert-gas condensation or magnetron sputtering. These techniques can be used only to obtain very small volumes of the materials. At the same time, there are several premises, which allow one to assume, that nanoglass state may be produced by means of severe plastic deformation (SPD).

It is known that deformation in amorphous ribbons, obtained by melt-spun, or bulk metallic glasses occurs by forming shear bands in amorphous phase, which leads to a certain structure transformation and properties changes [15–18]. In particular, some

* Corresponding author. Institute of Physics of Advanced Materials of Ufa State Aviation Technical University, 12 K. Marx str., Building 3, Room 3-117, Ufa 450000, Russia.
E-mail address: dimagun@mail.ru (D.V. Gunderov).

http://dx.doi.org/10.1016/j.intermet.2015.06.013
0966-9795/© 2015 Elsevier Ltd. All rights reserved.

studies showed the increase of BMG ductility after the preliminary deformation up to high strain values [19]. However, due to the low ductility of amorphous alloy, high strain is unable to achieve by conventional deformation methods (compression, tension, rolling). The SPD method such as HPT allows processing with very high strains even at low ductile materials, including amorphous alloys [20–22]. One can expect that in a certain amorphous alloys, high density of shear bands with increased free volume will be formed by means of HPT, that make the obtained structure similar to "nanoglasses". The goal of this work is the complex study of microstructure and properties of the amorphous Ti–Ni–Cu alloy, subjected to HPT at various temperatures, and determination the possibility of formation the structure like "nanoglasses" in such a way.

2. Material and methods

The initial ternary quasibinary $Ti_{50}Ni_{25}Cu_{25}$ alloy was manufactured by electric arc melting. The melt-spun was performed by spinning of a melt jet onto a rapidly rotating copper cylindrical cooler at a cooling rate of 10^6 K/s. The melt-spun (MS) ribbons with a thickness of 0.04 mm and a width of 2 mm were obtained as a result. To conduct HPT processing, the MS ribbons were cut into flakes (strips) with a length of 10 mm, which were then laid on the surface of the anvils in several layers. The HPT processing was carried out by torsion under a high pressure of 6 GPa at room temperature and at temperatures of 50, 100 and 150 °C. To produce the samples, 10 revolutions of the Bridgman anvils were performed at a rotation speed of 1 rev/min. Using such a technique, solid samples with a thickness of 0.2–0.3 mm and a diameter of 10 mm were obtained from melt-spun ribbons.

The material fine structure was investigated using the transmission electron microscope (TEM) JEM-2100 at an accelerating voltage of 160 and 200 kV. The foils for electron microscopy were produced on the twin jet polishing machine "Tenupol-5" by the standard method using an electrolyte 10%$HClO_4$ + 90%$CH_3(CH_2)3OH$ (90% of butanol). The voltage was 50 V at room temperature. Foil etching by argon ions was additionally carried out at JEOL IONSLICEREM-09100 15. TEM studies were conducted in the region of ½ radius of the HPT-processed sample.

The structure of the samples was investigated by X-ray diffraction under the Cu radiation at Bruker Phaser D2. The DSC tests were performed on a Netzsch DSC 204 F1 Phoenix calorimeter; the heating temperature was 520 °C and the typical heating rate was 20 °C/min.

To reveal mechanical properties, nanoindentation tests were performed at high-precision nanohardness scratch tester Nanovea. The measurement were made at Load = 150 mN; Loading Rate = 300 mN/min; Contact Load = 0.5 mN. Ten measurements were conducted on each state, whereby the mean values of elastic modulus were determined. The standard error of these measurements was about 12%. Nanoindentation tests were performed in the region of ½ radius of the HPT-processed sample.

3. Results and discussion

Fig. 1 shows the X-ray diffraction patterns of the produced samples. It is clear that melt-spun ribbons are mostly amorphous. According to the XRD patterns, structure of melt-spun ribbons subjected to HPT remains amorphous, significant changes in the amorphous phase structure by XRD after SPD could not be detected.

The TEM studies of initial melt-spun $Ti_{50}Ni_{25}Cu_{25}$ alloy microstructure, microdiffraction and the bright field image indicate the amorphous state at the site of the melt-spun ribbon (see Fig. 2a).

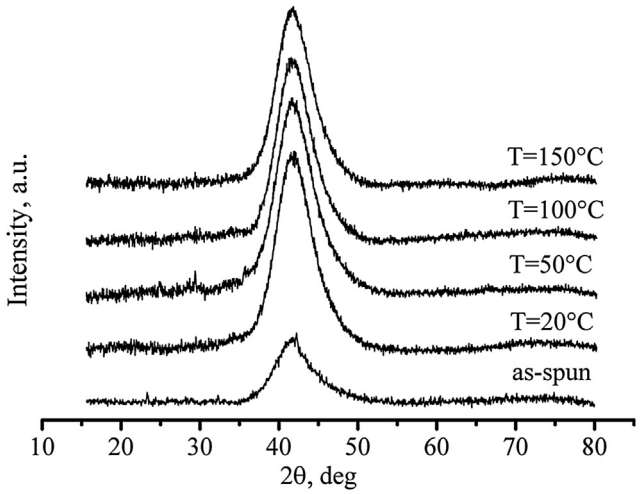


Fig. 1. The XRD diffraction patterns of initial melt-spun $Ti_{50}Ni_{25}Cu_{25}$ ribbon and melt-spun $Ti_{50}Ni_{25}Cu_{25}$ alloy after HPT n = 10 at different temperatures.

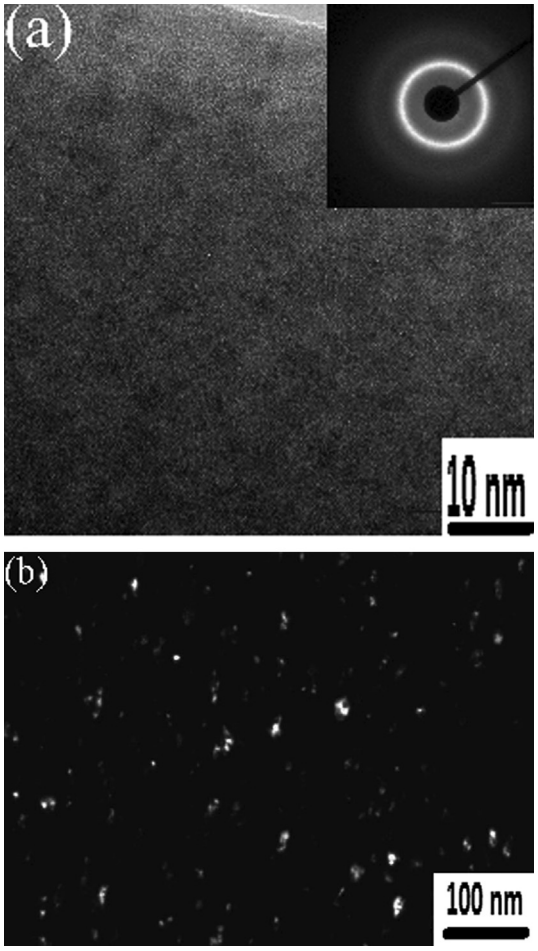


Fig. 2. The microstructure of the initial melt-spun $Ti_{50}Ni_{25}Cu_{25}$ alloy: a) the bright field image and microdiffraction from amorphous site; b) the dark field image from the site, where nanocrystals are presented.

However, single nanocrystals are observed in some areas of the dark field image (see Fig. 2b), which is probably due to heterogeneity of melt-spun ribbon. However, based on the XRD data, one may confirm that the majority of melt-spun ribbon is amorphous.

Fig. 3 shows the TEM picture of melt-spun $Ti_{50}Ni_{25}Cu_{25}$ alloy after HPT up to 10 revolutions at the temperature T = 20 °C. Microdiffraction and the bright field image indicate the amorphous state of alloy. Individual nanocrystals of 5 nm in size are displayed in the dark field in some sites; in other sites they are not observed. The light regions observable in the bright field are clusters of about 25 nm, separated by darker boundaries. Clusters are not observed in the dark field. The size of observed clusters in the bright field is visibly larger than the size of the nanocrystals, displayed in the dark field. Therefore, the clusters observed in the bright field are amorphous regions and are not nanocrystals.

Perhaps the observed picture can be interpreted as a structure of nanoglasses type – the nanoscale amorphous clusters of the same topology, separated by amorphous boundaries of another topology with increased free volume or different chemical compositions (chemical separation during HPT), whereas before the HPT structure is more homogeneous. Therefore, one can assume that HPT of amorphous alloy led to the formation of «nanoglass type structure». Nevertheless, this is only one possible explanation, and the nature of such a contrast requires further detailed studies. The TEM studies here show that the microstructure of melt-spun $Ti_{50}Ni_{25}Cu_{25}$ alloy after HPT up to 10 revolutions at the temperatures T = 50 °C and T = 100 °C are similar to the microstructure after HPT up to 10 revolutions at the room temperature.

The microstructure of $Ti_{50}Ni_{25}Cu_{25}$ alloy after HPT up to 10 revolutions at the temperature T = 150 °C has a number of features (Fig. 4). Microdiffraction indicates the amorphous state of the alloy. Nanocrystals are also displayed in the dark field images in greater numbers than after HPT at the room temperature. This is probably the result of some nanocrystallization activation due to higher temperature of HPT.

However, in case of HPT up to 10 revolutions at the temperature T = 150 °C observable in the bright field clusters are separated by lighter boundaries (Fig. 4a). One can notice that the size of the "clusters" is slightly greater (40 nm), and the boundaries between the "clusters" thinner and less blurred than in case of HPT up to 10 revolutions at the temperature T = 20 °C. Thus, one can assume that the difference between the structure of "amorphous clusters" and the structure of boundaries between the amorphous clusters became more distinct and the boundaries are identified more clearly with increase of the HPT temperature.

As one can see from Fig. 5, HPT processing at 20 °C leads to a decrease of the crystallization start temperature to 400 °C from 460 °C in the initial MS state. An increase of the HPT processing temperature leads to the growth of the crystallization start temperature from 400 °C for the sample deformed at 20 °C, up to 420 °C for the sample deformed at 150 °C. It is clear from Fig. 5 that the temperature range of the crystallization becomes more narrow for the samples deformed at the higher temperature. The less wide temperature range can prove that the structure of the samples becomes more homogeneous than in the case of lower deformation temperatures.

Table 1 shows the results of elastic modulus measurements of the melt-spun $Ti_{50}Ni_{25}Cu_{25}$ alloy in different states. Analysis of the nanoindentation results shows that the elastic modulus of the material (E) increased by approximately 20%, as a result of HPT processing for up to 10 revolutions at a temperature T = 20 °C in relation to the values in the initial melt-spun state (Table 1). By increasing the temperature of HPT to 100 °C and 150 °C, elastic modulus decreases. Previously, an increase of the elastic modulus was observed at HPT processing of bulk metallic glass [15]. In Ref. [15] the following explanation of the observed effect is given:

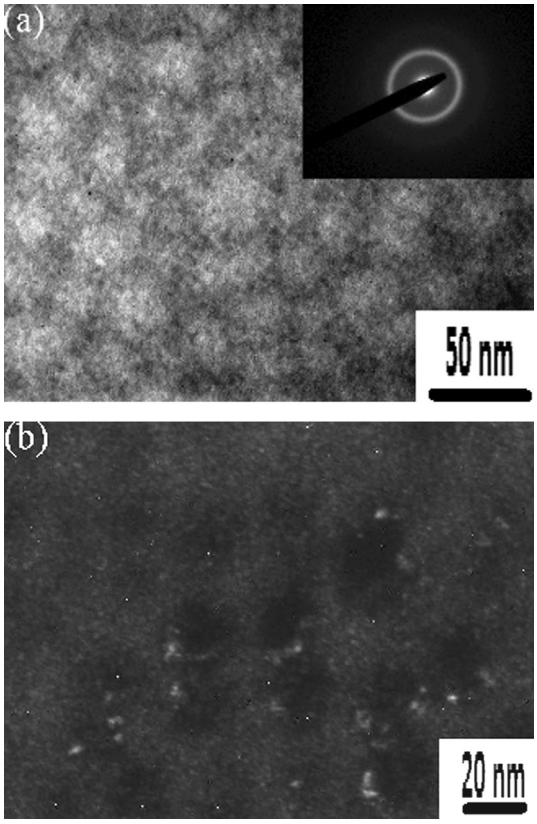


Fig. 3. The microstructure of melt-spun $Ti_{50}Ni_{25}Cu_{25}$ alloy after HPT up to 10 revolutions at the temperature T = 20 °C: a) the bright field image and microdiffraction; b) the dark field image.

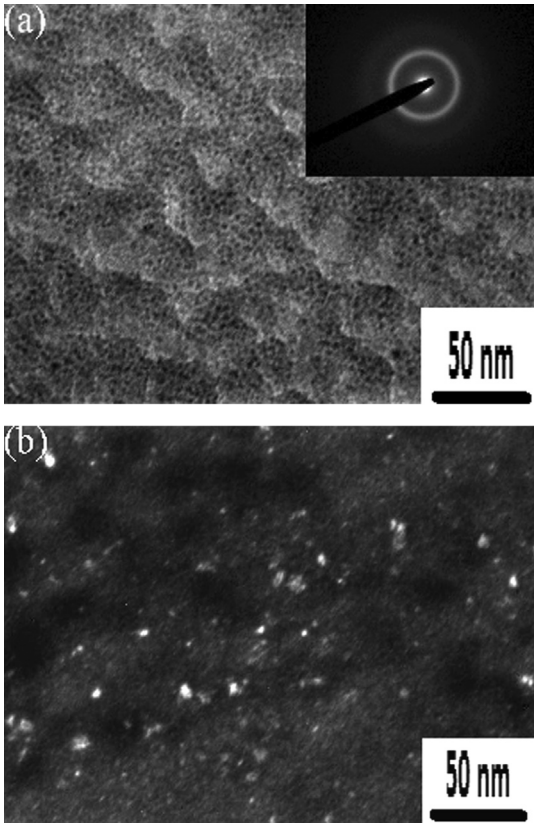


Fig. 4. The microstructure of $Ti_{50}Ni_{25}Cu_{25}$ alloy after HPT up to 10 revolutions at the temperature T = 150 °C: a) the bright field image and microdiffraction; b) the dark field image.

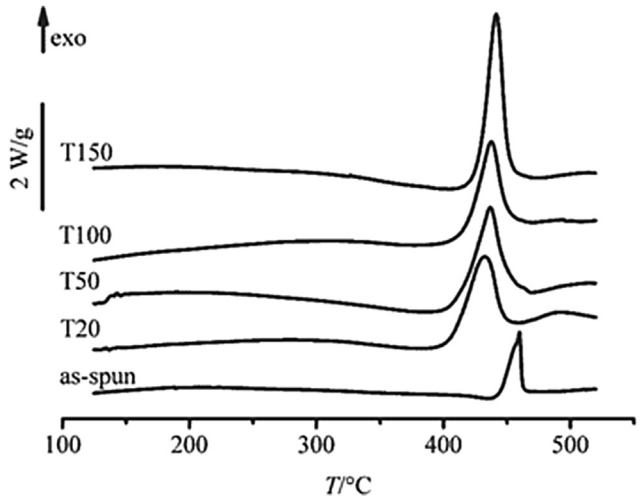


Fig. 5. DSC curves of as-spun and HPT-processed samples $Ti_{50}Ni_{25}Cu_{25}$ alloy.

As the atomic density in the nano-glass interfaces is reduced in comparison to a melt-quenched glass with the same chemical composition, the enhancement of the Young's modulus noted in all nano-glasses tested so far indicates that the interatomic interaction in nano-glasses differs from the interaction in the corresponding melt-quenched glass. Also, the glass regions of the nano-glass have an atomic arrangement that is indistinguishable from the one in the melt-quenched ribbon. Hence, it seems likely that the new electronic structure is associated with the interfaces between the glassy regions [15].

Thus, the comparison of the initial melt-spun ribbons and the HPT-processed amorphous alloy by several experimental techniques reveals the significant structural changes as well as big difference of mechanical behavior.

The nature of the contrast observed in the bright field images in the SPD-processed melt-spun ribbons, and observable “clusters” (regions separated by boundaries) is not quite clear by now. The observed contrast from the obtained data is different for the samples in different states: for the melt-spun ribbons, for the melt-spun ribbons after HPT up to 10 revolutions at the temperature T = 20 °C and the melt-spun ribbons after HPT up to 10 revolutions at the temperature T = 150 °C. Therefore, the specific contrast observed in the bright field images is associated with the structural state of the material.

As already mentioned, the deformation in amorphous phase occurs through the formation of shear bands. Based on the structural difference of melt-spun ribbons before and after HPT, one may assume that these changes are associated with the formation of high density of shear bands in the amorphous phase. The width of shear bands formed in amorphous phase during the strain is 10–30 nm [23], i.e. it is comparable to the size of observed “clusters”, and is much larger than the boundaries width between clusters. Single shear bands were not observed by TEM or SEM after HPT in amorphous alloys [19]. This is obviously due to the fact that shear bands are formed throughout the whole volume of the material and overlap each other during the HPT deformation with 5 and more revolutions.

Another important issue is defining the role of thermal heating during HPT processing. It should be noted that the glass transition temperature of MS TiNiCu amorphous alloy is about 320°C, the crystallization temperature is 450°C [24,25], which is noticeably higher than the highest employed temperature of HPT processing (150°C). However, heating during HPT processing can play in important role [26,27]. According to model calculations, during HPT processing of BMG $Cu_{60}Zr_{30}Ti_{10}$, the temperature may increase up to 650 K (380°C) [26]. On the other hand, according to some experimental studies, during HPT processing of metals the temperature increases only by 60–70°C [28], and temperature increase during deformation by HPT processing remains a debatable issue. Without any doubt, an important role in the structural transformations under HPT processing is played by free volume evolution during HPT and local structural variations near shear bands [27]. In particular, an increase in free volume during HPT and diffusion activation due to free volume leads, during the HPT processing of amorphous MS Nd-Fe-B alloys, to the immiscibility of the amorphous phase with precipitation in the amorphous phase of the α-Fe phase nanocrystals [21,29]. In the MS TiNiCu amorphous alloy, the immiscibility of the amorphous phase with precipitation of nanocrystals of pure metals does not take place during HPT processing, but there occurs HPT-induced nanocrystallization with formation of very small nanocrystals of the B2 phase, with a size of about 3 nm [21]. In the present paper, the main attention is focused on the fact that HPT processing of MS TiNiCu probably leads to an additional transformation of the amorphous phase with an appearance (according to the TEM bright-field image) of nanoscale amorphous clusters, separated by amorphous boundaries of another topology. Note should be made that the size and contrast of nanoscale amorphous clusters and amorphous boundaries depend on the temperature of HPT processing. Such structural transformations of the amorphous phase can be accounted for either by an increase in the temperature during deformation by HPT (however, this should lead primarily to crystallization), or by volume evolution during HPT [27], which can result in the free volume distribution between « nanoscale amorphous clusters» and «amorphous boundaries».

Table 1
The results of nanoindentation melt-spun $Ti_{50}Ni_{25}Cu_{25}$ alloy prior to and after HPT n = 10.

State	Initial ribbon	HPT T = 20°C	HPT T = 100°C	HPT T = 150 °C
Elastic modulus, GPa	110	140	140	120

4. Conclusion

In summary, it was shown that:

The comparison of the initial melt-spun ribbons and HPT-processed amorphous $Ti_{50}Ni_{25}Cu_{25}$ alloy reveals changes in their atomic structure and mechanical properties.

The structure formed as a result of HPT processing, can probably be described as nanoscale amorphous clusters separated by amorphous boundaries of another topology, and it may be interpreted as a structure of nanoglass type. The elastic modulus values are increased after HPT processing in relation to the values of the initial melt-spun state, which is also typical for the nanoglass state.

Accurate measurements are still needed to confirm or disprove this assumption and a detailed study will be carried out in the ongoing research.

Acknowledgements

The authors acknowledge gratefully the financial support of the structure research in this study, provided by the Russian Science Foundation through project № 14-12-00138. Mechanical testing was performed under the financial support of the Russian Ministry of Education and Science through project № 14.B25.31.0017. Structural studies (X-ray) were performed at the Research Centre

for X-ray Diffraction Studies and Interdisciplinary Resource Centre for Nanotechnology of St. Petersburg State University. Nanoindentation and TEM studies were performed using the equipment of the Common Use Center «Nanotech» of Ufa State Aviation Technical University: http://nanotech.ugatu.ac.ru/

References

[1] H. Gleiter, Nanostructured materials: basic concepts and microstructure, Acta Mater. 48 (2000) 1–29.
[2] R.Z. Valiev, Y. Estrin, Z. Horita, T.G. Langdon, M.J. Zehetbauer, Y.T. Zhu, Producing bulk ultrafine-grained materials by severe plastic deformation, JOM 58 (4) (2006) 33.
[3] R.Z. Valiev, M.J. Zehetbauer, Yu Estrin, et al., The innovation potential of bulk nanostructured materials, Adv. Eng. Mater. 9 (7) (2007) 527–533.
[4] R. Valiev, R. Islamgaliev, I. Alexandrov, Bulk nanostructured materials from severe plastic deformation, Prog. Mat. Sci. 45 (2000) 103–189.
[5] J.Y. Huang, Y.T. Zhu, X.Z. Liao, R.Z. Valiev, Amorphization of TiNi induced by high-pressure torsion, Philos. Mag. Lett. 84 (3) (2004) 183–190.
[6] A.V. Sergueeva, C. Song, R.Z. Valiev, A.K. Mukherjee, Structure and properties of amorphous and nanocrystalline NiTi prepared by severe plastic deformation and annealing, Mater. Sci. Eng. A.339 (1) (2003) 159–165.
[7] D. Gunderov, N. Kuranova, A. Lukyanov, V. Makarov, E. Prokofiev, A. Pushin, Structure and properties of aging and nonaging alloys $Ti_{49.4}Ni_{50.6}$ and $Ti_{50.2}Ni_{49.8}$ subjected to high pressure torsion, Rev. Adv. Mater. Sci. 25 (2010) 58–66.
[8] V.V. Stolyarov, D.V. Gunderov, A.G. Popov, V.S. Gaviko, A.S. Ermolenko, Structure evolution and changes in magnetic properties of strongly deformed Nd(Pr)–Fe–B alloys during annealing, J. Alloys Compd. 281 (1998) 69–71.
[9] V.V. Stolyarov, D.V. Gunderov, R.Z. Valiev, A.G. Popov, V.S. Gaviko, A.S. Ermolenko, Metastable states of nanostructural Nd(Pr)FeB alloys processed by severe plastic deformation, JMMM 196–197 (1999) 166–168.
[10] D.V. Gunderov, A.G. Popov, N.N. Schegoleva, V.V. Stolyarov, A.R. Yavary, Phase transformation in crystalline and amorphous rapidly quenched Nd–Fe–B alloys under SPD, in: M. Zehetbauer, R.Z. Valiev (Eds.), Nanomaterials by Severe Plastic Deformation, WILEY-VCH Verlag GmbH&Co. KGa, Weinheim, 2004, pp. 165–169.
[11] Adam Revesz, Sandor Hobor, Janos L. Labar, Alex P. Zhilyaev, Zsolt Kovacs, Partial amorphization of a Cu–Zr–Ti alloy by high pressure torsion, J. Appl. Phys. 100 (2006) 103522.
[12] M.F. Ashby, A.L. Greer, Metallic glasses as structural materials, Scr. Mater. 54 (2006) 321.
[13] H. Gleiter, Nanoglasses: a new kind of noncrystalline materials, Beilstein J. Nanotechnol. 4 (2013) 517–533.
[14] H. Gleiter, Nanoscience and nanotechnology: the key to new studies in areas of science outside of nanoscience and nanotechnology, MRS Bull. 34 (2009) 456–464.
[15] H. Gleiter, Th Schimmel, H. Hahn, Nanostructured solids-from nano-glasses to quantum transistors, Nano Today 9 (2014) 17–68.
[16] R.A. Andrievski, Metallic nano/microglasses: new approaches in nanostructured materials science, Phy. Usp. 56 (3) (2013) 261–268.
[17] VYu Zadorozhnyy, A. Inoue, D.V. Louzguine-Luzgin, Ti-based nanostructured low-alloy with high strength and ductility, Mater. Sci. Eng. A 551 (2012) 82–86.
[18] Q.S. Zhang, W. Zhang, G.Q. Xie, D.V. Louzguine-Luzgin, A. Inoue, Stable flowing of localized shear bands in soft bulk metallic glasses, Acta Mater. 58 (2010) 904–909.
[19] Fanqiang Meng, Koichi Tsuchiya, Seiichiro II, Yoshihiko Yokoyama, Reversible transition of deformation mode by structural rejuvenation and relaxation in bulk metallic glass, Appl. Phys. Lett. 101 (2012) 121914.
[20] X.D. Wang, Q.P. Cao, J.Z. Jiang, H. Franz, J. Schroers, R.Z. Valiev, Y. Ivanisenko, H. Gleiter, H.-J. Fecht, Atomic-level structural modifications induced by severe plastic shear deformation in bulk metallic glasses, Scr. Mater. 64 (2011) 81–84.
[21] R.Z. Valiev, D.V. Gunderov, A.P. Zhilyaev, A.G. Popov, V.G. Pushin, Nanocrystallization induced by severe plastic deformation of amorphous alloys, J. Metastable Nanocryst. Mater. 22 (2004) 21–26.
[22] V.G. Pushin, R.Z. Valiev, Y.T. Zhu, D.V. Gunderov, A.V. Korolev, N.I. Kourov, T.E. Kuntsevich, E.Z. Valiev, L.I. Yurchenko, Severe plastic deformation of melt-spun shape memory Ti_2NiCu and Ni_2MnGa alloys, Mater. Trans. 47 (3) (2006) 546–549.
[23] Y. Zhang, A.L. Greer, Thickness of shear bands in metallic glasses, Appl. Phys. Lett. 89 (2006) 071907.
[24] A.V. Pushin, A.A. Popov, V.G. Pushin, Effect of deviations of composition from the quasi-binary section TiNi–TiCu on structural and phase transformations in rapidly quenched alloys, Phys. Metal. Metallogr. 114 (8) (2013) 692–702.
[25] V.G. Pushin, N.N. Kuranova, A.V. Pushin, E.Z. Valiev, N.I. Kourov, A.E. Teplykh, A.N. Uksusnikov, Formation of nanocrystalline structure in the amorphous $Ti_{50}Ni_{25}Cu_{25}$ alloy upon severe thermomechanical treatment and the size effect of the thermoelastic martensitic B2 ↔ B19 transformation, Phys. Metal. Metallogr. 113 (3) (2012) 271–282.
[26] Sándor Hóbor, Zsolt Kovács, Ádám Révész, Macroscopic thermoplastic model applied to the high pressure torsion of metallic glasses, J. Appl. Phys. 106 (2009) 023531.
[27] Peter Henits, Adam Revesz, Zsolt Kovacs, Free volume simulation for severe plastic deformation of metallic glasses, J. Mech. Mater. 50 (2012) 81–87.
[28] Alexander Zhilyaev, Terence Langdon, Reassessment of temperature increase and equivalent strain calculation during high-pressure torsion, IOP Conf. Ser. Mater. Sci. Eng. 63 (2014) 1–7, 012052.
[29] Wei Li, Lanlan Li, Yun Nan, Zhenyu Xu, Xiangyi Zhang, A.G. Popov, D.V. Gunderov, V.V. Stolyarov, Nanocrystallization and magnetic properties of amorphous $Nd_9Fe_{85}B_6$ subjected to high-pressure torsion deformation upon annealing, J. Appl. Phys. 104 (2008) 023912.